Acta Chemica Scandinavica, 1996: 50: 580–586
Printed in UK – all rights reserved

ACTA
CHEMICA SCANDINAVICA
ISSN 0904-213X

Effect of Non-Stoichiometry on Properties of $La_{1-t}MnO_{3+\delta}$. I. Phase Relations

Natsuko Sakai† and Helmer Fjellvåg*

Department of Chemistry, University of Oslo, N-0315 Oslo, Norway

Sakai, N. and Fjellvåg, H. 1996. Effect of Non-Stoichiometry on Properties of $La_{1-t}MnO_{3+\delta}$. I. Phase Relations. – Acta Chem. Scand. 50: 580–586. © Acta Chemica Scandinavica 1996.

Phase-relation data for lanthanum manganese oxide, $La_{1-t}MnO_{3+\delta}$, with emphasis on lanthanum and oxygen non-stoichiometry, unit-cell dimensions and structure type are provided. The La deficiency covers the range $0.00 \geqslant t \geqslant 0.09 \pm 0.02$, and is mainly charge compensated by changes in the oxygen content. The maximum formal oxidation state of manganese is reduced rather than increased on increasing the La deficit. Quenching conditions for obtaining one of three structural modifications (RH, ORT1, ORT2), as well as the relationship between slowly cooled samples, quenched samples and samples studied under *in-situ*, controlled oxygen partial pressure conditions are described. Reoxidation during quenching is not important for air-equilibrated samples and $T < 1273$ K. However, samples subjected to reducing conditions prior to quenching tend partly to reoxidize. The first-order ORT1→ORT2→RH-type transitions are rapid, implying that the situation conveyed by quenched samples from specific $T,p(O_2)$ conditions differ from the *in-situ* equilibrium situation. Thermal expansion and phase-transition data are presented for the three modifications. On heating the Jahn–Teller deformed ORT1-type phase, the cooperative distortion is destroyed around 450–600 K. A pseudocubic phase, possibly of the ORT2-type, and the RH-type modification with regular MnO_6 octahedra, become stabilized. The transitions are connected with discontinuous volume contractions.

Lanthanum manganese(III) oxide, $LaMnO_3$, takes a distorted perovskite-type structure. It exhibits substantial non-stoichiometry, as indicated by the notation $LaMnO_{3+\delta}$. Variants substituted with alkaline earths $(La,M)MnO_{3+\delta}$, M=Ca and Sr, with high electronic conductivities have recently been repeatedly investigated owing to a technological interest in their use as cathode materials in solid oxide fuel cells (SOFC).[1] Ideally, the oxygen content $(3+\delta)$ of the perovskite would be 3.00 when the rare earth (RE) and 3*d*-metal ions are trivalent. However, manganese tends to oxidize into the tetravalent state. Experimental data strongly suggest that any introduced charge unbalance is compensated by vacancies at the La and Mn sites in equal proportions, which implies an increased nominal oxygen content.[2,3] The defect structures of such oxygen-excessive compounds have been studied by, e.g. thermogravimetric, electromotive force (EMF) and conductivity measurements.[4–9] The Seebeck coefficient, as well as the variation of non-stoichiometry with temperature and oxygen partial pressure, indicate a possible partial charge disproportionation of trivalent manganese into di- and tetravalent manganese.[7–9]

The wide range of non-stoichiometry results in intriguing structural, electric and magnetic properties. For example, whereas $LaMnO_3$ itself is a semiconductor, increased Mn^{IV} content favours metallic conduction.[5] For certain compositions a temperature induced metal–insulator transition occurs,[10] and antiferromagnetism in $LaMnO_3$ is converted into ferri- and ferromagnetism for samples with significant amounts of Mn^{IV}.[11] Also, the crystal structure is susceptible to the oxygen content, and changes from orthorhombic for $\delta=0$ to rhombohedral for $\delta=0.15$.[12]

The characteristics of lanthanum-deficient $La_{1-t}MnO_{3+\delta}$ were first reported by Shimoyama *et al.*[13] It shows an improved SOFC electrode performance owing to higher compatibility with the electrolyte, yttrium-stabilized zirconia (YSZ).[14–16] The alkaline-earth substituted $(La,M)_{1-t}MnO_{3+\delta}$ compounds (M= Ca or Sr) are popular electrode materials for SOFC, and the La-deficient materials show a very reduced tendency towards undesirable $La_2Zr_2O_7$ formation and exhibit improved catalytic activity and chemical stability under SOFC operating conditions.[17] The La deficit affects properties like unit-cell dimensions,[12] sinterability,[14,18]

† Present address: Department of Inorganic Materials, National Institute of Materials and Chemical Research, 1-1 Higashi, Tsukuba, Ibaraki 305, Japan.
* To whom correspondence should be addressed.

redox behaviour,[19,20] electrical conductivity[10,20] and also the quenching temperatures required for providing materials of either orthorhombic or rhombohedral type.[12]

From fundamental and applied points of view extended knowledge on the properties of $La_{1-t}MnO_{3+\delta}$ is desirable. The present series of papers aims at establishing correlations between composition, defect structure, average crystal structure, magnetic order and electronic properties. During the preparation of these, several papers on $LaMnO_{3+\delta}$ appeared.[21–25] Phase-relation data are presented in Part I, crystal structure data in Part II, magnetic and electronic properties, including magnetic structures, in Parts III and IV, and *in-situ* high-temperature powder neutron diffraction data in Part V. Several aspects are presently considered. The limits for La deficiency, and the effect of non-stoichiometry (t, δ) on the unit-cell dimensions are described. The relation between quenched samples and samples slowly cooled from specific temperature (T) – partial pressure [$p(O_2)$] conditions is discussed on the basis of high-temperature powder X-ray diffraction data, including *in-situ* studies. The operative chemical formula $La_{1-t}MnO_{3+\delta}$ is used, since the defect structure itself is not a main concern of the paper.

Experimental

Four sets of samples with nominal La contents, $t=0.00$, 0.04, 0.08 and 0.12, were prepared via a coprecipitation method. Aqueous solutions of $LaCl_3$ and $MnCl_2$, with concentrations determined by chelatometry, were used as starting reagents. These were mixed in appropriate amounts and dropped into an excess of ammonium carbonate solution, resulting in precipitation of carbonates. Since divalent manganese may form soluble amine complexes, the manganese content in the separated solution was measured by chelatometry. The loss of manganese was $<0.02\%$ of the total. The precipitated mixture of $La_2(CO_3)_3$ and $MnCO_3$ was washed thoroughly until no chloride was detected in the washing water by means of silver nitrate solution. The dried precipitates were calcined at 1373 K for 12 h in air to obtain oxide powders. Each sample was ground into a fine powder prior to further heat treatments.

Three kinds of $La_{1-t}MnO_{3+\delta}$ samples were prepared, termed respectively reduced, oxidized and quenched. The *reduced* samples were obtained by treatment in $CO_2/H_2/Ar$ gas mixtures. The oxygen potential was monitored with an yttrium-stabilized zirconia sensor and kept at $p(O_2)=10^{-7}$ Pa at 1273 K for 6 h, under which conditions there is no decomposition into La_2MnO_4 and MnO. The subsequent cooling was performed while keeping the ratio of the gas mixture unchanged. The sample compositions were assumed as $La_{1-t}Mn^{III}O_{3-1.5t}$, i.e. with solely trivalent manganese, assumptions which are based on extensive data in the literature.[4,20] The *oxidized* samples were obtained after final annealing in air at 1023 K for 2 d with subsequent slow cooling to room temperature. The *quenched* samples were prepared by first treating the samples in a thermogravimetric (TG) apparatus (Perkin Elmer, TGA7) at a selected temperature (873–1623 K) in O_2 flow. The samples were annealed for 1–24 h after constant weight was reached, before finally taken out in oxygen and quenched into liquid nitrogen at a cooling rate of around 200 K s^{-1}.

The oxygen contents of *oxidized* samples were established by oxidizing the corresponding *reduced* samples (with known/assumed compositions, see above) to the oxidized state. This was done by annealing some 150 mg of a reduced sample in the TG apparatus at 1273 K in O_2 flow. The flow was kept during the subsequent cooling to 298 K in order to obtain oxygen saturation. Maximum weight was obtained around 850 K. An example of the recorded weight change is given in Fig. 1. The quenched samples were analyzed in a related way; (i) the composition prior to quenching at the quenching temperature, T_q, was assessed from the weight change occurring on further heating above the maximum weight situation (which served as reference level), and (ii) the composition of samples after quenching was derived from reoxidation into the maximum weight situation.

Phase purity, homogeneity and unit-cell dimensions were evaluated from powder X-ray diffraction (PXD) data at 298 K [Guinier–Hägg camera, Cu $K\alpha_1$ radiation, Si as internal standard; $a=543.1065$ pm]. Unit-cell dimensions were deduced on the basis of about 15 Bragg reflections by means of the CELLKANT program.[26] The LAZY PULVERIX program[27] was used as aid in correct indexing of reflections for the orthorhombic unit cell with pseudocubic metric. All samples were characterized by SEM/EDX (scanning electron microscopy/energy-dispersive X-ray analysis; S-800, Hitachi Co. Ltd., Japan/Kevex Co. Ltd., USA).

High-temperature PXD data were collected with a Siemens D500 diffractometer for the temperature range 473–1173 K at various oxygen potentials [$p(O_2)$]. Gas mixtures of O_2[$p(O_2)=10^5$ Pa] and $H_2/CO_2/Ar$ [$p(O_2)=10^{-7}$ Pa at 1073 K] were flowed through the measuring chamber, and a $Zr(Y)O_2$ sensor was used to analyze $p(O_2)$ of the exhaust gas. The PXD profiles were analyzed by the Rietveld technique, using the DBW3.2S program[28] in order to obtain the most correct unit-cell dimensions and at the same time achieve verification of the structure type. A Guiner–Simon camera was used for two-dimensional visualization of temperature-induced changes in Bragg positions. The sample (ca. 5 mg) was kept inside closed (ca. 1 mm^3) or open silica glass capillaries. Cu $K\alpha_1$ radiation was used. The temperature was varied between 300 and 1200 K, and the temperature change was synchronized with movement of the film cassette.

Results and discussion

(i) Non-stoichiometry. For $0.00 \geqslant t \geqslant 0.08$, PXD shows a one-phase situation. The analyzed oxygen contents for oxidized ($3+\delta_{ox}$) and reduced ($3+\delta_{red}$) samples are

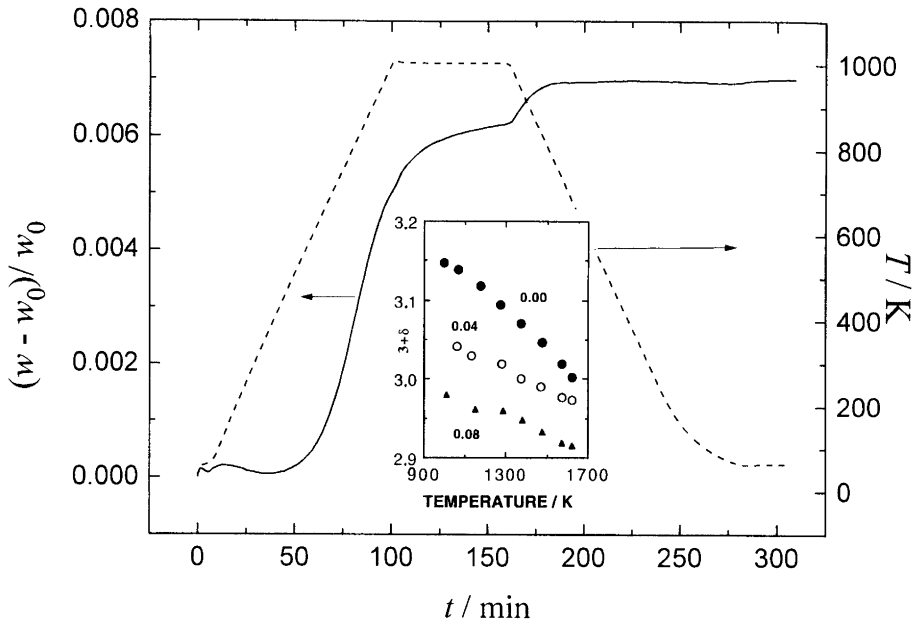

Fig. 1. Weight change of reduced $La_{0.92}MnO_{3+\delta}$ (solid line) during reoxidation in O_2. The initial oxygen content of the sample is assumed to be $3-1.5t=2.88$. Maximum weight is obtained around 850 K. The dotted line refers to the temperature profile during TGA experiments. The inset shows the oxygen content, $3+\delta$, for $La_{1-t}MnO_{3+\delta}$ analyzed by TGA in 1 atm O_2.

given in Table 1. The range of oxygen non-stoichiometry decreases with increasing nominal La deficit. Formally seen, the reduced positive charge in the unit cell on increasing t, is not compensated by further Mn^{IV} formation but by reduced oxygen excess. Mizusaki *et al.*[20] reported that the average manganese valency (v_{Mn}) is constant (3.30–3.35) irrespective of the La deficit. The results in Table 1 suggest a reduction of v_{Mn} with t, in line with wet chemical analysis data by Krogh-Andersen *et al.*[29] This controversy may just reflect the fact that different conditions were chosen for oxygen saturation, annealing at 600 °C vs. slow cooling. The apparently larger non-stoichiometry for $t=0.12$ (Table 1) is not intrinsic to $La_{1-t}MnO_{3+\delta}$. For the $t=0.12$ samples, lack of achievement of constant weight during TG treatment, a reddish brown colouring of the Al_2O_3 crucible, SEM/EDX tracing of particles with anomalously high manganese contents (Fig. 2), as well as powder X-ray and neutron diffraction data proved precipitation of manganese oxides. The upper limit for La deficit is considered as $t=0.09\pm0.02$.

Table 1. Oxygen content, $3+\delta$, of $La_{1-t}MnO_{3+\delta}$ as determined thermogravimetrically.

t	$3+\delta_{red}$	$3+\delta_{ox}$	Upper average Mn valency
0.00	3.00	3.14	3.28
0.04	2.94	3.05	3.22
0.08	2.88	2.98	3.20
0.12[a]	2.82	2.95	3.26

[a] Impurities observed.

(ii) Unit-cell dimensions at 298 K. Three structural modifications were confirmed; one rhombohedral ($LaAlO_3$-type, space group $R\bar{3}c$, here termed RH-type) and two orthorhombic (both $GdFeO_3$-type, space group *Pnma*), one of which showing a Jahn–Teller distorted structure owing to Mn^{III} high spin atoms ($a>c$; termed ORT1-type), the second having pseudocubic metric ($a\approx b/\sqrt{2}\approx c$; termed ORT2-type). Quenching conditions, oxygen contents and unit-cell dimensions are listed for selected quenched RH-, ORT1- and ORT2-type samples in Table 2. Included are also data for reduced and oxidized samples.

Within the three groups of oxidized, quenched and reduced samples, changes in the La deficit cause small yet significant variations in the unit-cell dimensions. The variations as a function of t are much less than expected on the basis of molar volumes, which must be rooted in a rather peculiar defect/vacancy situation.

For constant t, the unit-cell volume decreases with increasing Mn^{IV} content (δ): e.g. for $t=0.00$ the volume reduction is $\Delta V/Z\Delta\delta\approx16\times10^6$ pm^3. Krogh Andersen *et al.*[29] ascribed this contraction to differences in Mn^{IV}–O and Mn^{III}–O bond lengths. The same observation is presently done for *quenched* samples, for which the unit-cell volume increases on going from the more oxidized to more reduced samples (i.e. going from low towards higher quenching temperatures, t fixed; see Table 2). The variation in unit-cell volume with quenching temperature is shown in Fig. 3 for $t=0.04$. The volume change of 1.5×10^6 pm^3 per formula unit ($Z=4$) between 1100 and 1650 K in Fig. 3 gives a calculated $\Delta\delta\approx0.10$. The data in Fig. 3 refer to RH-, ORT2- and ORT1-type samples,

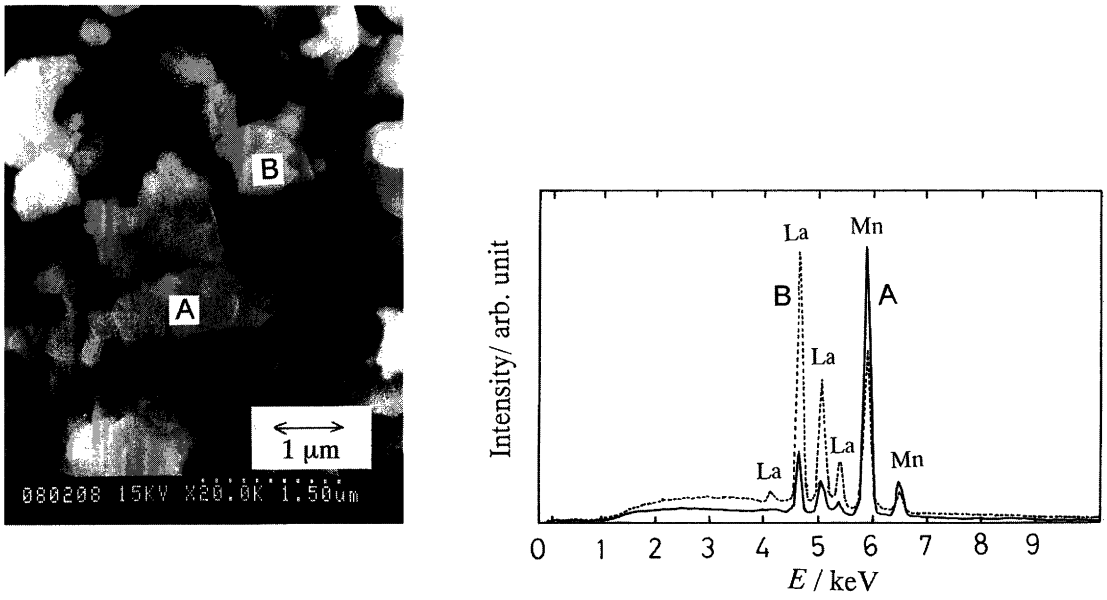

Fig. 2. SEM image and EDX profile of a powder sample with nominal composition $La_{0.88}MnO_{3+\delta}$ calcined in air at 1373 K. The two-phase situation is illustrated by the white grain (A) having a much larger manganese content than the surrounding grain (B).

Table 2. Unit-cell dimensions at 298 K for selected, quenched (in pure O_2), oxidized and reduced samples of $La_{1-t}MnO_{3+\delta}$.[a]

t	T_q/K	Time/h	Type	a/pm	b/pm	c/pm	α/°	$V/10^6$ pm^3	$3+\delta$
0.00	995	24	RH	556.4			60.70	234.39(6)	
	1093	24	ORT2	548.7	777.8	553.1		236.02(11)	
	1279	16	ORT2	550.5	779.4	553.2		237.35(8)	
	1484	3	ORT2	551.3	780.3	552.2		237.50(6)	
	Oxidized		RH	546.7			60.73		3.15
	Reduced		ORT1	573.4	770.3	554.0		244.71(8)	3.00[b]
0.04	1093	24	RH	547.2			60.66	235.21(5)	
	1283	16	RH	548.2			60.68	236.52(10)	3.022
	1481	2	ORT2	550.4	781.4	553.8		238.18(17)	3.01
	1632	1	ORT1	563.7	772.4	554.2		241.24(11)	
	Oxidized		RH	547.4			60.64		3.05
	Reduced		ORT1	573.7	769.0	553.7		244.26(12)	2.944
0.08	1089	24	RH	547.4			60.59	235.05(6)	2.95
	1293	11	RH	548.3			60.63	236.43(5)	2.94
	1479	2	ORT2	548.7	781.1	553.5		237.22(17)	2.93
	1634	1	ORT1	560.9	773.4	554.0		240.29(11)	
	Oxidized		RH	547.6			60.58		2.98
	Reduced		ORT1	572.9	769.5	553.4		243.97(9)	2.88[b]

[a] Annealing time, quenching temperature (T_q) and structural modification (RH-, ORT1-, ORT2-type) are given. Calculated standard deviations in a, b, c and α are one or two in the last digit. The volumes refer to the orthorhombic structure types ($V_{ORT}=2\ V_{RH}$; $Z=4$; calculated standard deviations in parentheses). Analyzed oxygen contents, $3+\delta$, from reoxidation by TGA given. [b] Assumed, see Experimental.

but no major discontinuity seems to arise in $V(T)$ owing to the change of structure type (cf. section iv). This probably reflects the rather few observation points in Fig. 3 and the fact that the variation in volume is dominated by changes in oxygen content. The La-deficient samples show a larger increase in unit-cell volume with T_q than that observed for $t=0.00$.

Removal of La atoms has a slight influence on the Mn oxidation state for the oxidized samples (Table 1), and hence only a small volume change is expected. The oxidized samples with $t=0.00$, 0.04 and 0.08 have increasingly Mn^{III} contents as indicated by the nominal valencies 3.28, 3.22 and 3.20, respectively, which is consistent with the observed increase in unit-cell volume, from 234.8×10^6 pm^3 for $t=0.00$ to 235.3×10^6 pm^3 for $t=0.04$. The modest volume (and axial) contraction which occurs for reduced samples ($La_{1-t}MnO_{3-t/2}$; ca. 100% Mn^{III}), from 244.7 for $t=0.00$ to ca. 244.0×10^6 pm^3 for $t=0.08$, is ascribed to vacancies at the La sublattice.

The unit-cell dimensions and their variation for the reduced samples appears at first sight as quite different from the reported situation with 1.1% change for the a-

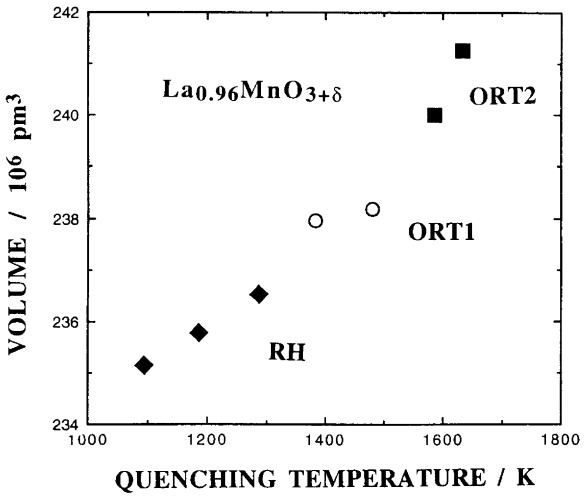

Fig. 3. Unit-cell volume as a function of quenching temperature for $La_{0.96}MnO_{3+\delta}$.

axis between $t=0.00$ and 0.10.[11] This discrepancy is probably rooted in sample preparation. Takeda *et al.*[11] reported $a \approx 567$, $b=772$ and $c \approx 553.5$ pm for reduced $LaMnO_3$ quenched in air from 1300 °C, which matches nicely results presently obtained for a sample heated in reducing atmosphere and quenched in air (into liquid nitrogen) from 973 K, $a=568.7(2)$, $b=771.0(2)$ and $c=554.0(1)$ pm. On the other hand, when such a sample is slowly cooled from 1300 to 300 K while keeping the reducing atmosphere, $a=573.38(9)$, $b=770.32(15)$ and $c=554.04(13)$ pm. This clearly demonstrates that the strongly reduced ORT1-type samples tend to reoxidize during quenching in air. The volume variation reported by Takeda *et al.*[11] may result from a composition dependent tendency for reoxidation (e.g. in oxygen diffusitivity).

These observations address the question of whether studies of quenched samples are of real significance. The variation of the oxygen stoichiometry in O_2 with temperature is shown for $La_{1-t}MnO_{3+\delta}$, $t=0.00$, 0.04 and 0.08, in the inset to Fig. 1. This should be compared with the analyzed oxygen contents for quenched samples in Table 1. For temperatures below 1273 K, the oxygen contents are equal, whereas at 1473 K the reoxidation during quenching increases δ by 0.02. Yasuda *et al.*[30] estimated from tracer measurements the oxygen diffusitivity in $LaMnO_{3+\delta}$ as 1×10^{-12} cm^2 s^{-1} (at 1273 K in O_2). Calculations on that basis are in reasonable agreement with the observed reoxidation. At higher temperatures the diffusitivity will be much larger. Hence, the state of samples obtained for $T_q > 1300$ K will to a large extent be determined by parameters like cooling rate and particle size. The very low tendency of $LaMnO_{3+\delta}$ to reoxidize at lower temperature, e.g. in comparison with reduced $LaCoO_{3-\delta}$, is rooted in the defect structure. For $LaMnO_{3+\delta}$ the oxygen sublattice is (nearly) perfect, whereas for $LaCoO_{3-\delta}$ it contains large numbers of vacancies.

(iii) Phase relations for quenched samples. The conditions required to obtain either of three modifications of $La_{1-t}MnO_{3+\delta}$ on quenching are given in Fig. 4. The findings concur with Takeda *et al.*[11] The depicted situation is not necessarily representative for the equilibrium situation at the quenching temperature (section iv), but may reflect subsequent reoxidation (for high T_q) and phase transitions. The border between RH- and ORT2-type regions increases from 1073 to 1373 K with increasing t, indicating that the La deficit favours the RH-type. The Jahn–Teller deformed samples are obtained on quenching from conditions where the Mn^{III} content is large; however, the cooperative deformation takes place at temperatures far below T_q.

(iv) High-temperature powder X-ray diffraction. PXD data (Guinier–Simon) show that the Jahn–Teller-deformed $LaMnO_{3.00}$ sample (ORT1-type; in sealed capillary), converts around 700 K into an intermediate, pseudocubic phase via a first-order phase transition. Temperature-induced changes in unit-cell dimensions are shown in Fig. 5. On further heating, another first-order transition around 820 K, converts the sample into RH-type, Fig. 5. The transitions ORT1 → intermediate → RH are connected with discontinuous volume contractions, Fig. 5.

When heating quenched samples of the ORT2-type, definite line splittings of the Bragg reflections develop above 500 K, showing the appearance of the RH-type. The splitting develops continuously; however, from symmetry reasons the ORT2- to RH-type transition is of first order, cf. $LaCrO_3$.[31]

Within the resolution of the Guinier–Simon technique,

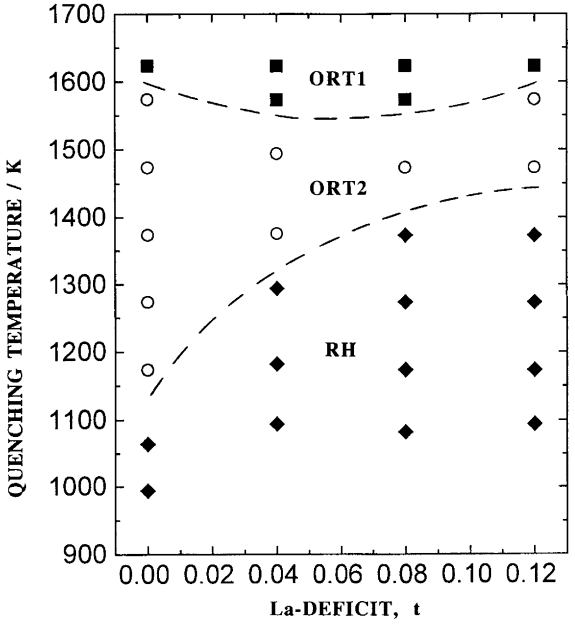

Fig. 4. Phase relations for $La_{1-t}MnO_{3+\delta}$ quenched in O_2. Occurrence regions (quenching temperature vs. composition t) for three modifications of $La_{1-t}MnO_{3+\delta}$ are given.

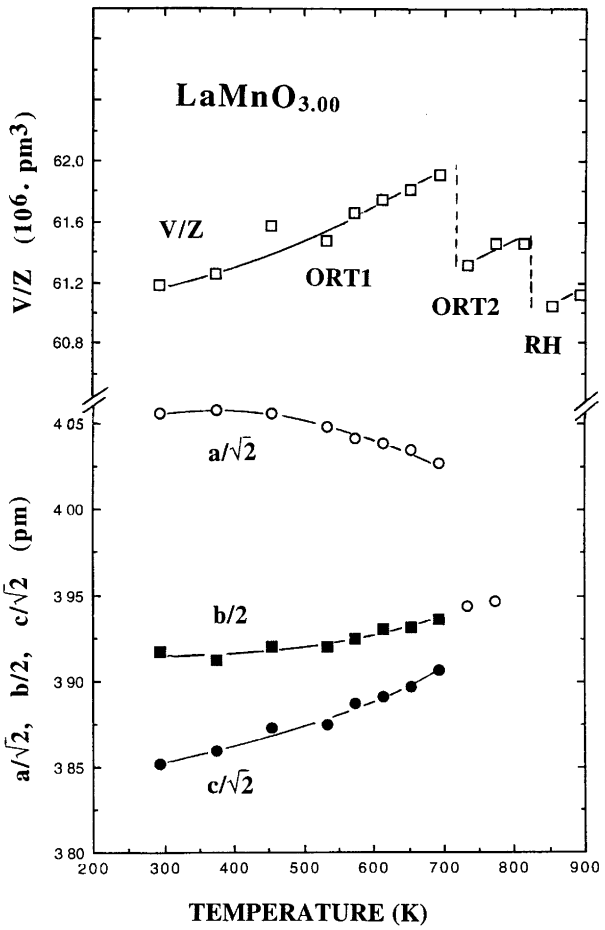

Fig. 5. Unit-cell dimensions as a function of temperature for reduced $LaMnO_{3+\delta}$, $\delta \approx 0.00$, heated inside a closed capillary. For the ORT2-type, see text.

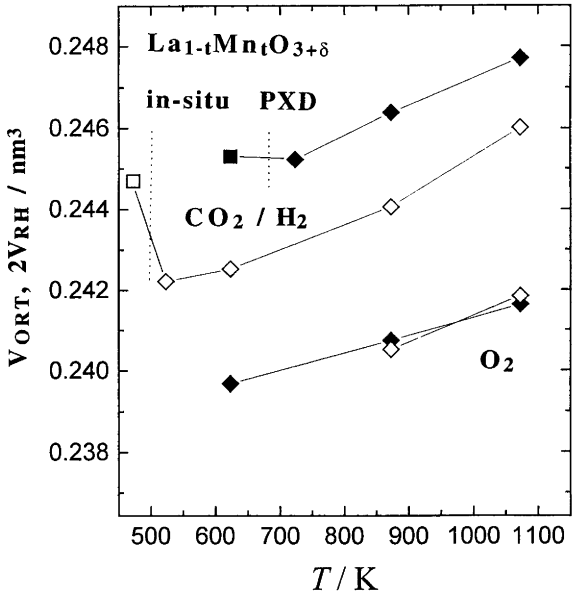

Fig. 6. Unit-cell volume as a function of temperature for $La_{1-t}MnO_{3+\delta}$, $t=0.00$ (open symbols) and 0.04 (closed symbols), under *in-situ* conditions in pure oxygen and in a CO_2/H_2 gas mixture. Squares ORT1-type, diamonds RH- or ORT2-type; for ORT2-type, see text.

no deviations from cubic metric could be identified for the intermediate phase. It should be noted that Hervieu *et al.*[21] recently described $LaMnO_{3+\delta}$ with 33% Mn^{IV} as cubic on the basis of electron diffraction data; however, the intermediate phase under present consideration has $3+\delta \approx 3.00$. Furthermore, the ORT2-type structure may for certain compositions attain pseudocubic metric; cf. the ratios from Table 2: $a/c \approx 1.004$ and $b/\sqrt{2}c \approx 1.003$. (Tilted octahedra give rise to substantial internal distortion.[31])

The equilibrium situation brought about by *in-situ* PXD for $t=0.00$ and 0.04 is somewhat different from that derived on the basis of quenched samples. Data for unit-cell volume and structure type in O_2 and CO_2/H_2 atmospheres [$p(O_2)=10^5$ Pa and 10^{-7} Pa at 1073 K, respectively] are shown in Fig. 6. In O_2 the samples are of the RH-type between 600 and 1100 K, and there is no discrepancy between quenched and *in-situ* samples. In a $CO_2/H_2/Ar$ atmosphere the *in-situ* samples are of the ORT1-type at low temperatures. On heating, phase transitions occur at 450 K and 650 K for $t=0.00$ and 0.04, respectively, whereas quenched samples (say $T_q=800$ K) are always of the ORT1-type. The *in-situ* studies show furthermore that a two-phase mixture of RH- and intermediate-type (possibly ORT2-type) phases occurs for $t=0.00$ and $450<T<650$ K. Above 650 K only the RH-type prevails. Rietveld analysis of PXD intensity data could be done satisfactory when describing the intermediate phase as being of the ORT2-type. For that reason the intermediate phase is named ORT2 in Figs. 5 and 6. For the reduced samples the phase-transition sequence appears to be the same for *in-situ* and closed capillary experiments. The transition observed at 620–700 K (vacuum) in heat-capacity data for $LaMnO_{3+\delta}$ measured by the laser flash method corresponds to the ORT1- to ORT2-/RH-type transition.[32] The structural phase transition shows further up as a clear change in magnetic susceptibility for $LaMnO_{3.00}$ in the same temperature interval.[33]

Acknowledgment. This work has received financial support from the Research Council of Norway.

References

1. Minh, N. Q. *J. Am. Ceram. Soc. 76* (1993) 563.
2. Tofield, B. C. and Scott, W. R. *J. Solid State Chem. 10* (1974) 183.
3. van Roosmalen, J. A. M., Cordfunke, E. H. P. and Helmholdt, R. B. *J. Solid State Chem. 110* (1994) 100.
4. Kuo, J. H., Anderson, H. U. and Spalin, D. M. *J. Solid State Chem. 83* (1989) 62.
5. Kuo, J. H., Anderson, H. U. and Spalin, D. M. *J. Solid State Chem. 87* (1990) 55.
6. Mizusaki, J., Tagawa, H., Naraya, K. and Sasamoto, T. *Solid State Ionics 49* (1991) 111.
7. van Roosmalen, J. A. M. and Cordfunke, E. H. P. *J. Solid State Chem. 110* (1994) 109.

8. Stevenson, J. W., Nasrallah, M. M., Anderson, H. U. and Spalin, D. M. *J. Solid State Chem. 102* (1993) 175.
9. Stevenson, J. W., Nasrallah, M. M., Anderson, H. U. and Spalin, D. M. *J. Solid State Chem. 102* (1993) 185.
10. Verelst, M., Rangavittal, N. and Rao, C. N. R. *J. Solid State Chem. 104* (1993) 74.
11. Hauback, B. C., Fjellvåg, H. and Sakai, N. *J. Solid State Chem. In press.*
12. Takeda, Y., Nakai, S., Kojima, T., Kanno, R., Imanishi, N., Shen, G. Q., Yamamoto, O., Mori, M. and Abe, T. *Mater. Res. Bull. 26* (1991) 153.
13. Shimoyama, J., Mizusaki, J. and Fueki, K. presented at the Fall Meeting of Chem. Soc. Jpn., Nagoya, Japan (1989) 3Q06.
14. Dokiya, M., Sakai, N., Kawada, T., Yokokawa, H., Iawata, T. and Mori, M. *Proceedings 24th Intersociety Energy Conversion Engineering Conference*, Vol. 3, p. 1547, Institute of Electrical and Electronics Engineers, New York 1989.
15. Yokokawa, H., Sakai, N., Kawada, T. and Dokiya, M. *Denki Kagaku, 57* (1989) 829.
16. Yokokawa, H., Sakai, N., Kawada, T. and Dokiya, M. *J. Electrochem. Soc. 138* (1991) 2719.
17. Kawada, T., Sakai, N., Yokokawa, H. and Dokiya, M. *Solid State Ionics 50* (1992) 189.
18. van Roosmalen, J. A. M., Cordfunke, E. H. P. and Huijsmans, J. P. P. *Solid State Ionics 66* (1993) 285.
19. Otoshi, S., Sasaki, H., Ohnishi, H., Hase, M., Ishimaru, K. and Ippommatsu, M. *J. Electrochem. Soc. 138* (1991) 1519.
20. Mizusaki, J., Tagawa, H., Yonemura, Y., Minamiue, H. and Nambu, H. In Worrell, W. L. and Tuller, H. L., Eds. *Proc. 2nd Int. Symp. on Ionic and Mixed Conducting Ceramics*, Ramaranayanan, T. A., *Electrochem. Soc. Proc. 94–12* (1994) 402.
21. Hervieu, M., Mahesh, R., Rangavittal, N. and Rao, C. N. R. *Eur. J. Solid State Inorg. Chem. 32* (1995) 79.
22. Ferris, V., Brohan, L., Ganne, M. and Tournoux, M. *Eur. J. Solid State Inorg. Chem. 32* (1995) 131.
23. Mahesh, R., Kannan, K. R., and Rao, C. N. R. *J. Solid State Chem. 114* (1995) 294.
24. van Roosmalen, J. A. M., van Vlaanderen, P., Cordfunke, E. H. P., Ijdo, W. L. and Ijdo, D. J. W. *J. Solid State Chem. 114* (1995) 516.
25. Norby, P., Krogh Andersen, I. G., Krogh Andersen, E. and Andersen, N. H. *J. Solid State Chem. 119* (1995) 191.
26. Ersson, N. O. *Program CELLKANT*, Department of Chemistry, University of Uppsala, Uppsala, Sweden 1981.
27. Yvon, K., Jeitschko, W. and Parthé, E. *J. Appl. Crystallogr. 10* (1977) 73.
28. Wiles, D. B. *Program for Rietveld Analysis of X-Ray and Neutron Diffraction Patterns: DBW3.2S*, Georgia Institute of Technology, Atlanta, GA 1982.
29. Krogh Andersen, I. G., Krogh Andersen, E., Norby, P. and Skou, E. *J. Solid State Chem. 113* (1994) 320 and personal communication.
30. Yasuda, I., Hishinuma, M., Kawada, T. and Dokiya, M. *121* (1996) 202.
31. Sakai, N., Fjellvåg, H. and Hauback, B. C. *J. Solid State Chem. In press.*
32. Kobayashi, M., Satoh, H. and Kamegashira, N. *J. Alloys Compounds, 192* (1993) 93.
33. Kamata, K., Nakajima, T., Hayashi, T. and Nakamura, T. *Mater. Res. Bull. 13* (1978) 49.

Received September 15, 1995.